Numerical modelling of sorption kinetics

Armando Coco

Department of Mathematics and Computer Science, University of Catania

Collaborators:
C. Astuto (KAUST, Saudi Arabia), G. Russo (Univ. of Catania)

workshop PRIN 2017 - Catania, 22 February 2023

Innovative Numerical Methods for Evolutionary Partial Differential Equations and Applications

Contents

Section 1

Introduction and Motivation

Contents

Introduction

The trapping of diffusing particles by a static or a moving trap is interesting in several contexts:

- chemistry
- physics
- biology

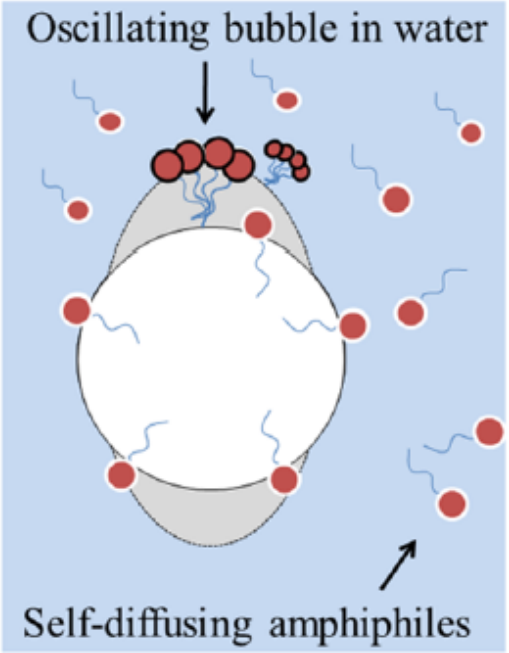

In biology, the application is to the study of the dynamics of self-diffusing amphiphiles attracted by a cell boundary.

Molecules like water on one side and fat on the other.
To better understand the phenomenon, a sort of scaled model has been built up as a reproducible and tunable biomimetic experimental model system to simulate a similar effect in laboratory [1].

[1] Oscillations of Bubble Shape Cause Anomalous Surfactant Diffusion: Experiments, Theory, and Simulations. A. Raudino, D. Raciti, A. Grassi, M. Pannuzzo, and M. Corti

Experimental setup

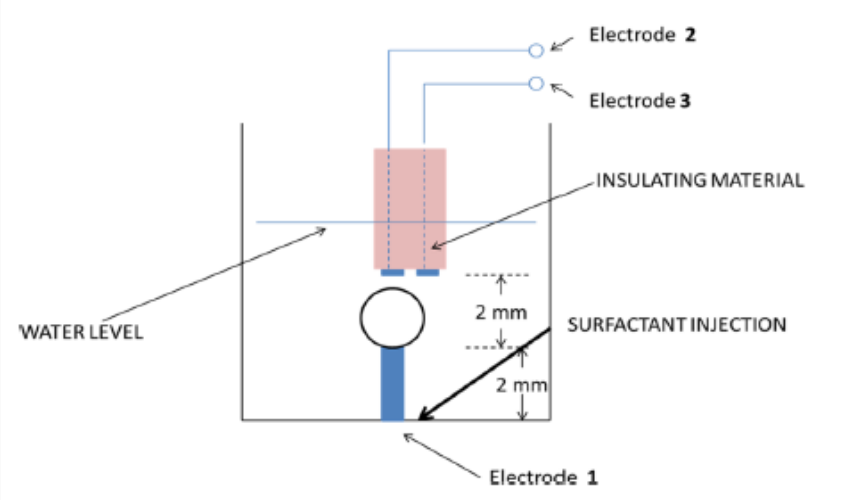

Figure 1: *Real (left panel) and schematic (right panel) setup of the experimental apparatus. The central sphere mimics the oscillating bubble.*

- The bubble is formed at the top of a stainless-steel tube protruding out from the bottom of a small square cell.
- A stream of *charged surfactant* diffuses around it, and (reversibly) binds to the bubble surface.
- Surfactants (anions) are partially soluble in water because of their polar head, and they prefer to settle at the bubble surface (hydrophobic repulsion between apolar tails and bulk water).

Measurements

Laboratory experiments provide evidence of a non monotone behavior in time of the concentration of particles by a detector located behind the bubble, under suitable experimental condition.

The effect of the bubble on the surfactant diffusional flow has been investigated. Results are summarized in the figure where the conductivity data in the absence of the bubble (red curve) are compared to those obtained by introducing a fixed bubble surface saturated by charged surfactants (blue curve). A different and unexpected behavior is observed when we introduce an empty **bubble oscillating at resonance frequency** (black curve).

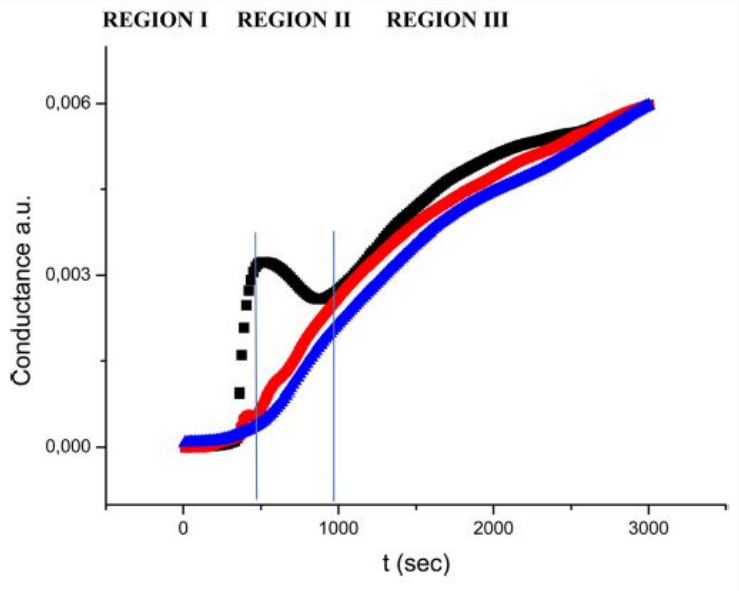

A comprehensive explanation of the phenomenon is not yet fully available.
Long term objective of the project is to provide a quantitative explanation of the phenomenon through numerical modelling.

multi-scale challenges

- Size of the bubble: about **1 mm in diameter**
- Attractive-repulsive potential of the bubble is of the order of $\leq 1\mu m$
- Bubble oscillations are excited at controlled amplitudes by a periodic electric field (thanks to the effective net charge at water-air interface) with voltage of a few tens of a millivolt, inducing oscillations of the order of to a **few hundredth of a nanometer**
- Typical frequencies: **100-200 Hz**
- Diffusion time and duration of the experiment of the order of **one hour**.

Section 2

Multiscale modeling of bubble-surfactants

Contents

Deduction of the reduced model in 1D

The numerical simulation of the system presents a multi-scale spatial challenge:

- the range of the bubble potential is confined within a few microns
- bubble radius is of the order of a millimeter

For this reason, a **reduced model** is proposed[1].

We start describing the model in 1D first.

The time evolution of a local concentration of ions $c = c(\vec{x}, t)$ diffusing in a steady fluid is governed by the conservation law

$$\frac{\partial c}{\partial t} + \frac{\partial J}{\partial x} = 0, \quad J = -D\left(\frac{\partial c}{\partial x} + \frac{1}{k_B T}\, c\, V'\right).$$

where k_B is the Boltzmann's constant, T is the absolute temperature and $V = V(\vec{x})$ is a suitable attractive-repulsive potential that models the particle trap.

[1] C. Astuto, A. Raudino and G. Russo

The domain of the problem is: $\Omega^\varepsilon = \Omega_b^\varepsilon \cup \Omega_f^\varepsilon = [-\varepsilon, \varepsilon L] \cup [\varepsilon L, 1] = [-\varepsilon, 1]$ with boundary conditions $J(-\varepsilon) = J(1) = 0$.

Assume that the trap is located at $x = 0$ and there is a wall at $x = 1$.

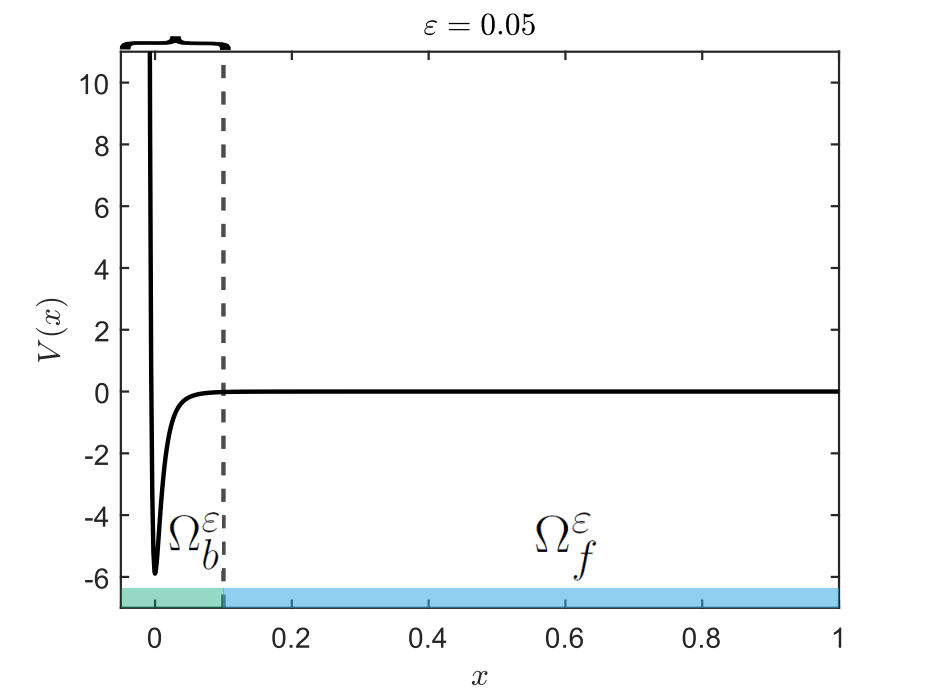

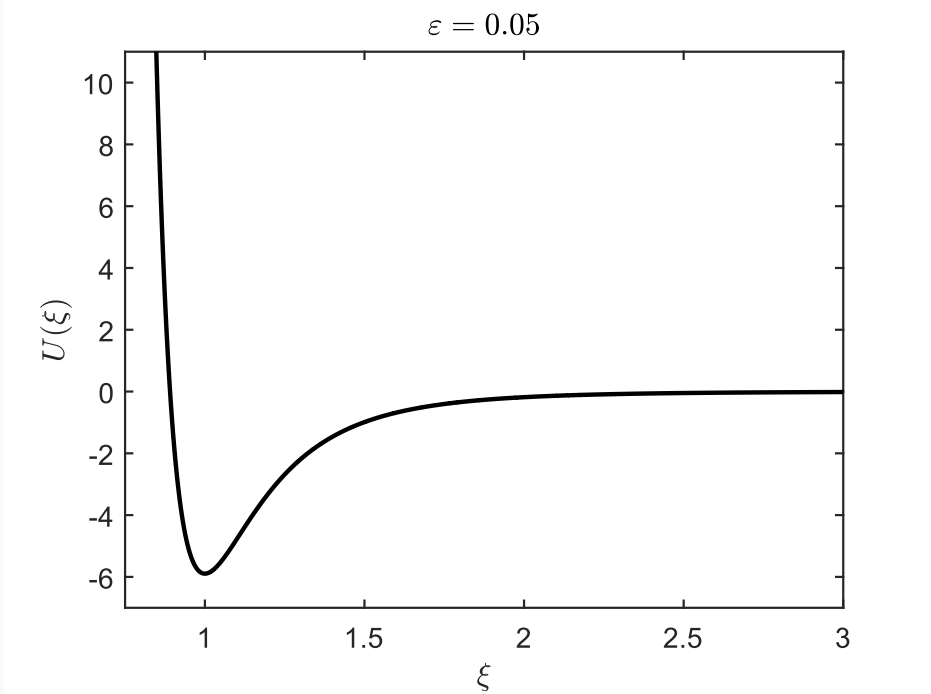

Aim: approximating the behaviour of the trap in Ω_b^ε with a suitable boundary condition at $x = 0$, obtaining then a simplified problem in $\Omega = [0, 1]$.

Using a scaling variable $\xi = 1 + x/\varepsilon$, the potential can be written in terms of $U(\xi)$ for $\xi \in [0, 1 + L]$ as $V(x) = U(\xi)$.

We assume that the solution $c_\varepsilon(\xi, t)$ of the scaled problem

$$\frac{\partial c_\varepsilon}{\partial t} + \frac{1}{\varepsilon}\frac{\partial J_\varepsilon}{\partial \xi} = 0, \quad J_\varepsilon = -D\frac{1}{\varepsilon}\left(\frac{\partial c_\varepsilon}{\partial \xi} + \frac{1}{k_B T}\, c_\varepsilon\, U'\right) \tag{1}$$

has the following expansion in Ω_b^ε:

$$c_\varepsilon(\xi, t) = c^{(0)}(\xi, t) + \varepsilon c^{(1)}(\xi, t) + O(\varepsilon^2). \tag{2}$$

Since the flux J_ε must be bounded for $\varepsilon \to 0$, from (1) we have that the coefficient of the term $\mathcal{O}(\varepsilon^{-1})$ in J_ε has to vanish:

$$\frac{\partial c^{(0)}}{\partial \xi} + \frac{1}{k_B T} U'(\xi) c^{(0)} = 0. \tag{3}$$

This equation can be solved for $c^{(0)}(\xi, t)$, yielding

$$c^{(0)}(\xi, t) = c^{(0)}(1 + L, t) \exp\left(-\frac{U(\xi)}{k_B T}\right) \tag{4}$$

since $U(1 + L) = 0$.

Integrating the conservation law

$$\frac{\partial c_\varepsilon}{\partial t} + \frac{1}{\varepsilon}\frac{\partial J_\varepsilon}{\partial \xi} = 0, \quad J_\varepsilon = -D\frac{1}{\varepsilon}\left(\frac{\partial c_\varepsilon}{\partial \xi} + \frac{1}{k_B T}\, c_\varepsilon\, U'\right)$$

in Ω_b^ε we have:

$$\frac{d}{dt}\int_{-\varepsilon}^{\varepsilon L} c(x,t)\, dx + J(\varepsilon L) - J(-\varepsilon) = 0$$

and using the approximation $c(x,t) \approx c^{(0)}(\xi,t)$, the boundary condition $J(-\varepsilon) = 0$ and that $V'(\varepsilon L) = 0$ we obtain

$$\varepsilon\, \frac{\partial c(\varepsilon L, t)}{\partial t} \int_0^{1+L} \exp\left(-\frac{U(\xi)}{k_B T}\right) d\xi - D\frac{\partial c(\varepsilon L, t)}{\partial x} = 0$$

that represents a boundary condition of $c(x,t)$ at $x = \varepsilon L$. Using this boundary condition at $x = 0$ instead of $x = \varepsilon L$, we finally obtain:

$$\boxed{M\frac{\partial c}{\partial t} - D\frac{\partial c}{\partial x} = 0 \quad \text{at } x = 0,} \quad \text{where } M = \varepsilon \int_0^{1+L} \exp\left(-\frac{U(\xi)}{k_B T}\right) d\xi. \tag{5}$$

We observe that:

- $M \to 0$ as $\varepsilon \to 0$ and then the condition (5) reduces to a zero Neumann boundary condition, therefore the interesting multiscale limit is obtained by letting $\varepsilon \to 0$, still maintaining M finite.

Extension of the condition to 2D and 3D

The condition seen before can be extended to 2D.

$$M\frac{\partial c}{\partial t} = MD\frac{\partial^2 c}{\partial s^2} - D\frac{\partial c}{\partial n}$$

and 3D:

$$M\frac{\partial c}{\partial t} = MD\Delta_\perp c - D\frac{\partial c}{\partial n}$$

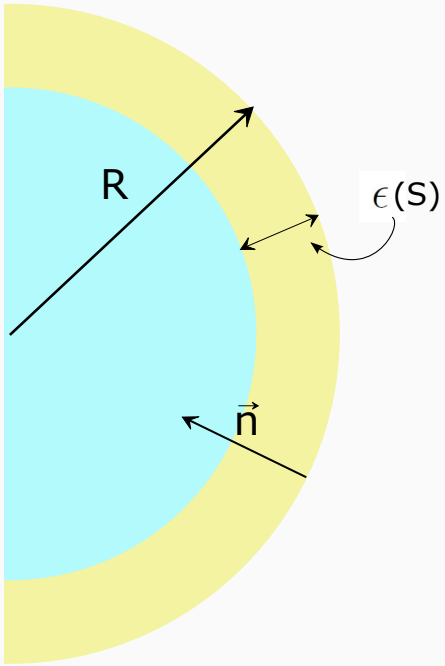

$$\text{with } M(s) = \varepsilon(s)\int_0^1 \exp\left(-\frac{\chi}{D}\left(U\left(R+\xi\varepsilon(s), s\right)\right)\right) d\xi$$

Reduced multiscale model

Let $\mathcal{B}$ be a circle centered in $(0,0)$ with radius equal to r, $\Omega = [-1,1]^2 \setminus \mathcal{B}$ be the computational domain. We rewrite the reduced model:

$$\frac{\partial c}{\partial t} = D\Delta c \quad \text{in } \Omega$$

$$\frac{\partial c}{\partial \hat{n}_{\mathcal{S}}} = 0 \quad \text{on } \Gamma_{\mathcal{S}}$$

$$M\frac{\partial c}{\partial t} = MD\frac{\partial^2 c}{\partial s^2} - D\frac{\partial c}{\partial \hat{n}_{\mathcal{S}}} \quad \text{on } \Gamma_{\mathcal{B}}$$

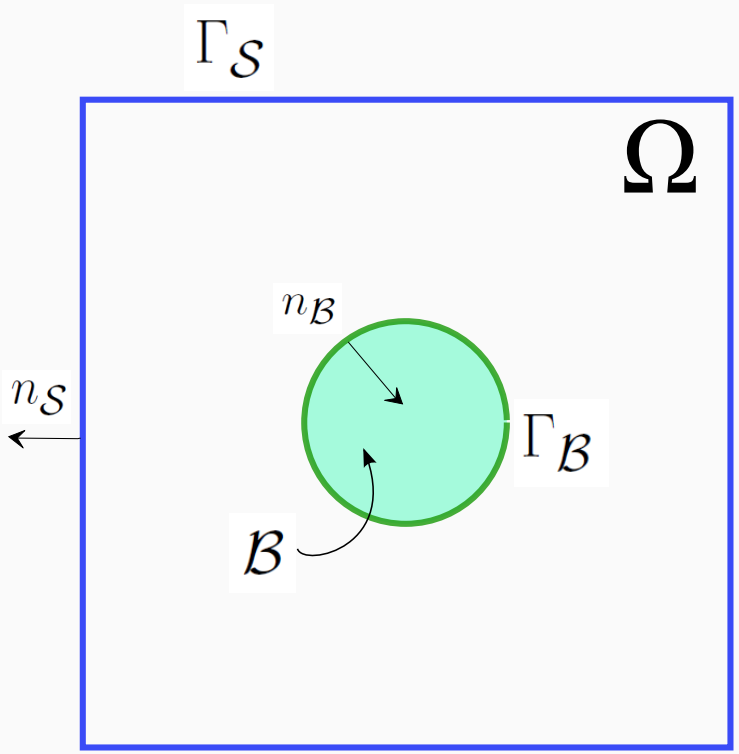

Section 3

Numerical discretization

Numerical discretization

The model problem can be written in compact form

$$\frac{\partial c}{\partial t} = Q\,c \tag{6}$$

where Q is the following (linear) differential operator

$$Q\,c = \begin{cases} D\Delta c & \text{in } \Omega \\ D\dfrac{\partial^2 c}{\partial \tau^2} - DM^{-1}\dfrac{\partial c}{\partial n} & \text{on } \Gamma_{\mathcal{B}} \end{cases}$$

Eq. (6) is discretized in time by using the Crank-Nicolson method, which is second order accurate:

$$\frac{c^{n+1} - c^n}{k} = \frac{1}{2}\left(Q\,c^n + Q\,c^{n+1}\right)$$

$$\left(I - \frac{k}{2}Q\right)c^{n+1} = \left(I + \frac{k}{2}Q\right)c^n \tag{7}$$

where k is the time step and I is the identity operator.

The operator $Q\,c$ is discretized on a uniform Cartesian grid by:

- standard 5-point stencil finite difference for the differential operators on internal points
- ghost-point technique for the boundary conditions on ghost points

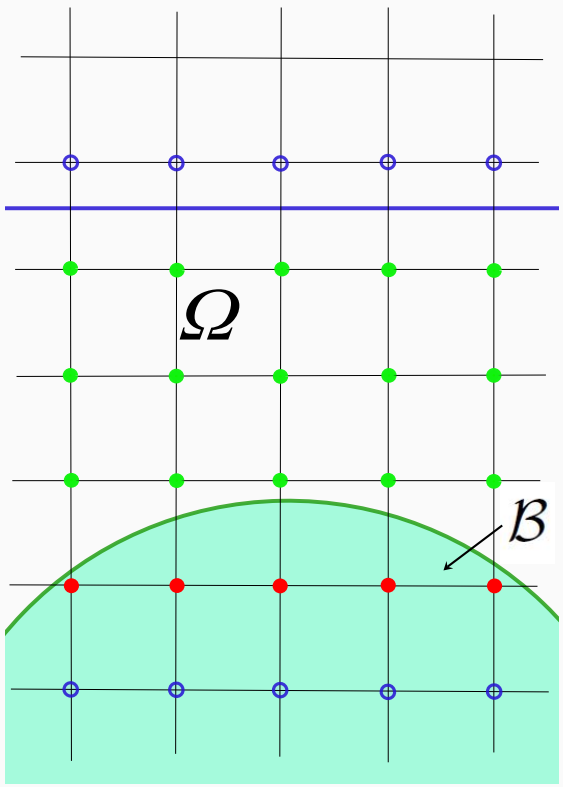

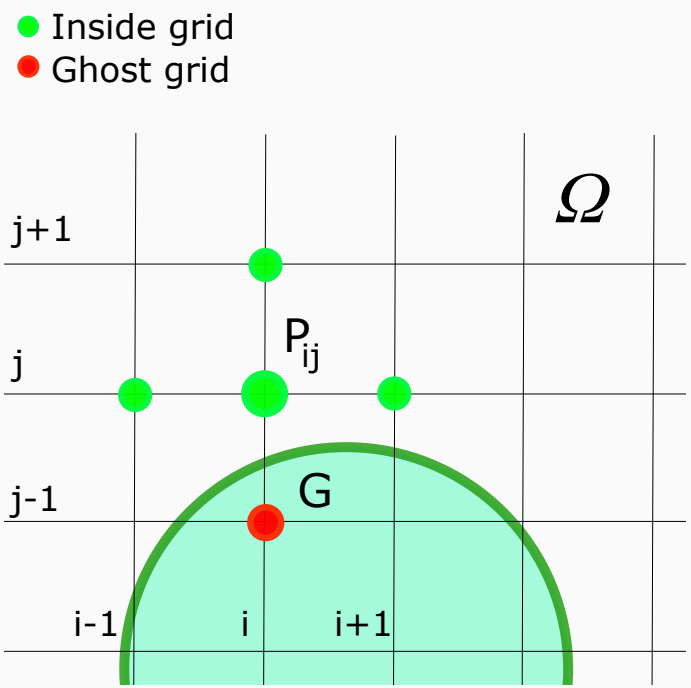

Spatial discretization of ghost points

The domain and the circle $\mathcal{B}$ are implicitly known by a level set function (signed distance function) $\phi(r,z) = R - \sqrt{r^2+z^2}$.

For each ghost point G, we compute the closest boundary point B by the signed distance function:

$$B = G - \vec{n}\cdot\phi(G), \quad \vec{n} = \nabla\phi.$$

The ghost value is obtained by discretizing $Q\,c$ as $Q\,\tilde{c}(B)$, where $\tilde{c}$ is a biquadratic interpolation on the following Upwind 9-point stencil:

(A.C., G. Russo (J. Comput. Phys. 2013, 2018))

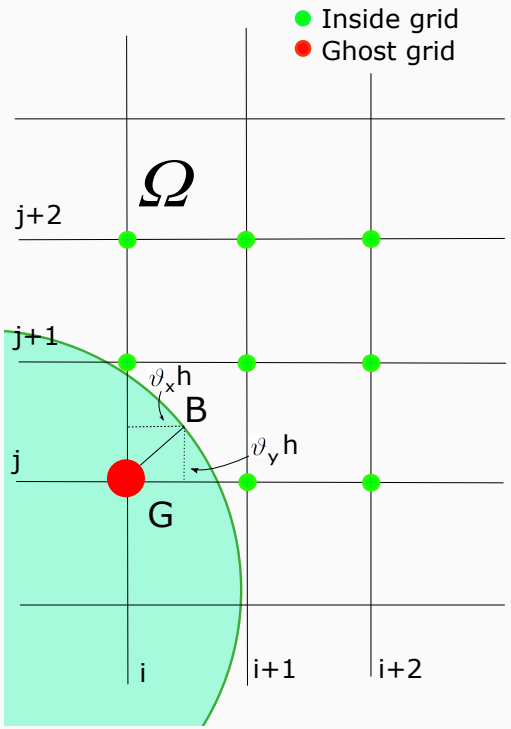

Key features of the method

- Equations for ghost points are coupled each other and cannot be easily eliminated from the internal equations
- The entire discretization results in a linear system containing both internal and ghost values as unknowns:

$$A_h\, c_h^{n+1} = b_h, \text{ where } A_h = \left(I_h - \frac{k}{2} Q_h\right) \text{ and } b_h = \left(I_h + \frac{k}{2} Q_h\right) c_h^n.$$

- The linear system is not symmetric, nor positive definite (due to the ghost values)
- It can be solved by a suitably adjusted multigrid approach [2]

[2] A.C., G. Russo (J. Comput. Phys., 2013)

Multigrid in brief

A multigrid method is an iterative solver that consists of the following algorithm:

Step 1. Perform ν_1 steps of a suitable relaxation scheme to the linear system $A_h\, c_h^{n+1} = b_h$, obtaining an approximated solution $\tilde{c}_h^{n+1}$

Step 2. Compute the residual $r_h = b_h - A_h \tilde{c}_h^{n+1}$

Step 3. Transfer the residual to a coarser grid with spatial step $H = 2h$ by: $r_H = \mathcal{I}_H^h r_h$

Step 4. Solve the residual equation: $A_H e_H = r_H$ (recursively!)

Step 5. Transfer the error e_H to the fine grid by: $e_h = \mathcal{I}_h^H e_H$

Step 6. Update the approximate solution: $\tilde{c}_h^{n+1} \leftarrow \tilde{c}_h^{n+1} + e_h$

Step 7. Perform ν_2 steps of the relaxation scheme to the linear system $A_h\, c_h^{n+1} = b_h$

$\longrightarrow$ Multigrid works if the relaxation scheme has the smoothing property.

Relaxation scheme

The relaxation scheme is:

$$c_h^{n+1,k+1} = c_h^{n+1,k} + P_h^{-1}(b_h - A_h c_h^{n+1,k}) \tag{8}$$

where P_h is a suitable *preconditioner*.

A standard Gauss-Seidel scheme corresponds to $P_h = (D_h + L_h)$, where D_h and L_h are the diagonal and lower part of A_h, respectively.

It does not converge!

Idea: we change the diagonal values of D_h that corresponds to ghost points, obtaining a new diagonal matrix $\tilde{D}_h$ whose values are:

$$\tilde{D}_h^{(i,j)} = \begin{cases} D_h^{(i,j)} = 1 + \dfrac{2kD}{h^2} & \text{if} \quad (x_i, y_j) \in \Omega_h \\ \beta & \text{if} \quad (x_i, y_j) \in \text{ Ghost} \end{cases}$$

where $\beta \in \mathbb{R}$ is a suitable value to be determine.

The iteration on a ghost point reads:

$$c_{i,j} \leftarrow c_{i,j} + \beta^{-1}\left(b_{i,j} - \left(I_h^{(i,j)} c_h - \frac{k}{2} Q_h^{(i,j)} c_h\right)\right)$$

that is

$$c_{i,j} \leftarrow \left(1 - \beta^{-1}\left(I_h^{(i,j),(i,j)} - \frac{k}{2} Q_h^{(i,j),(i,j)}\right)\right) c_{i,j} + \ldots \text{ terms independent of} c_{i,j} \ldots$$

The value β is chosen in such a way that

$$\left|1 - \beta^{-1} A_h^{(i,j),(i,j)}\right| \leq 1, \text{ with } A_h^{(i,j),(i,j)} = \left(I_h^{(i,j),(i,j)} - \frac{k}{2} Q_h^{(i,j),(i,j)}\right).$$

$$\Longrightarrow \ldots \Longrightarrow |\beta| \geq \frac{1}{2}\left(1 + \frac{Dk}{2}\left(\frac{13}{2h^2} + \frac{3}{|M|\, h}\right)\right).$$

This is the convergence criterion. However, it usually degrades the multigrid performance (boundary effects).

Optimal multigrid

There are two strategies to overcome boundary effects:

→ add a few extra boundary relaxations on the ghost points per internal relaxation.

→ Determine the optimal relaxation parameter β per each ghost point

(A.C., M. Mazza, M. Semplice; J. Comput. Phys., 2023):

$$\beta_{\text{OPT}} = \beta(\phi)$$

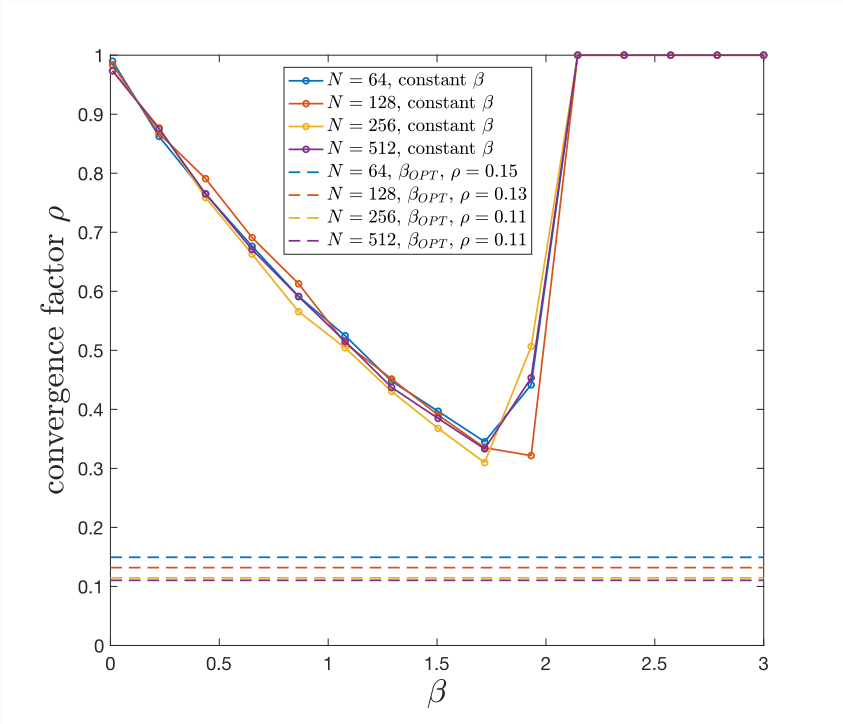

Restriction operator: $r_H = \mathcal{I}_H^h r_h$

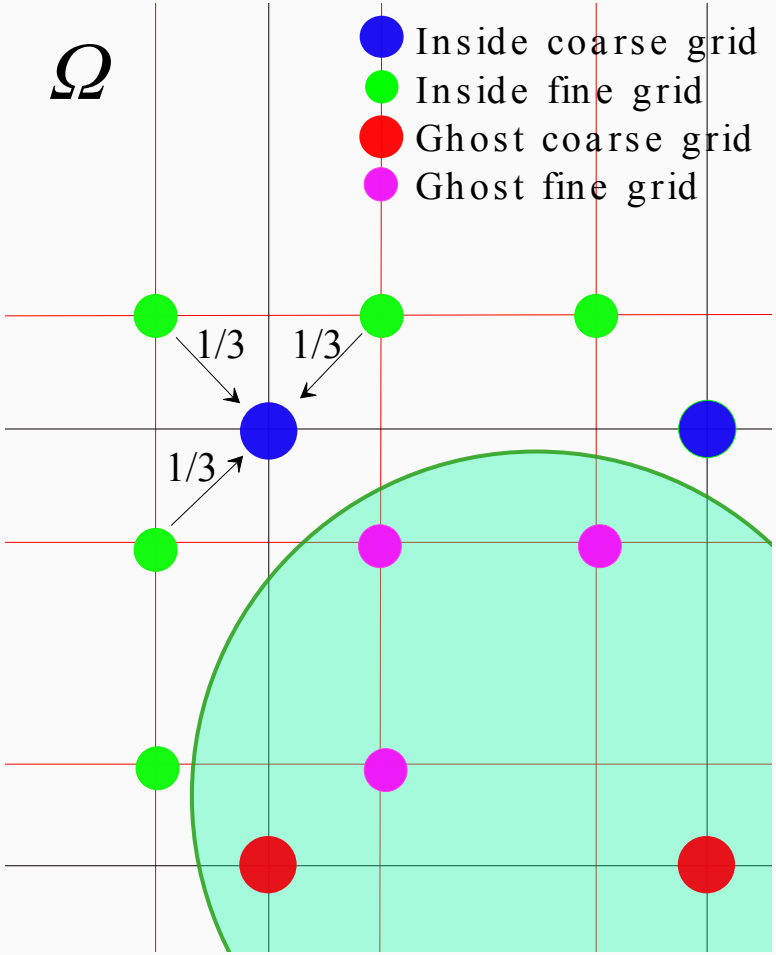

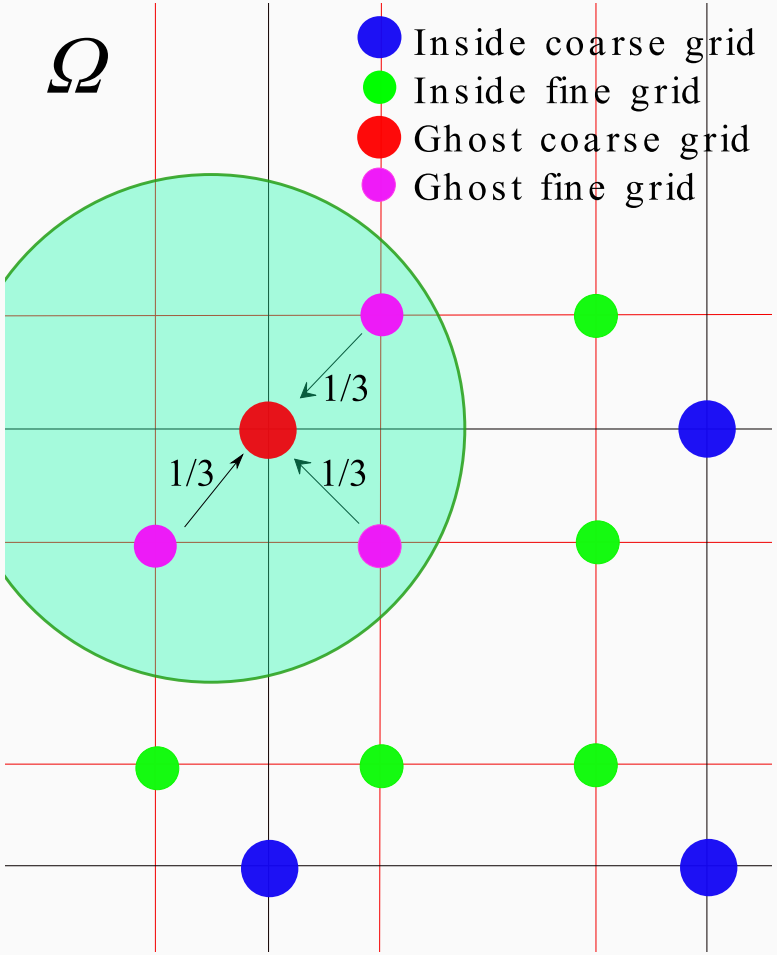

Interpolation operator: $e_h = \mathcal{I}_h^H e_H$

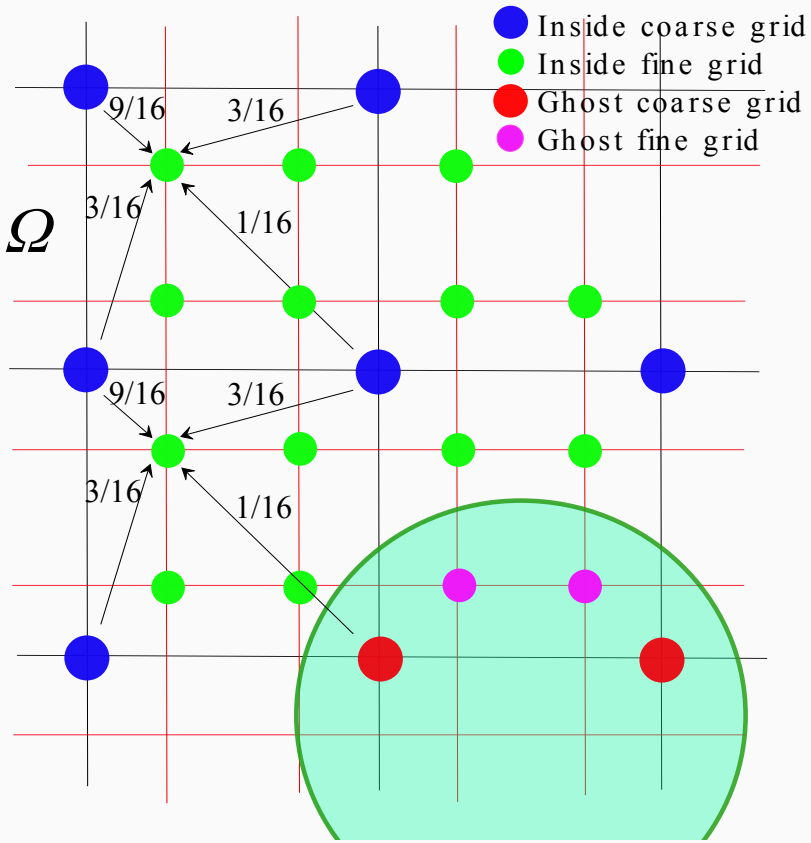

Accuracy tests

Second order accuracy in space and time is tested. We choose an "ad hoc" solution $c_{exa}(r, z, t)$ and add suitable sources f and g.

Exact solution:

$$c_{exa}(r, z, t) = \cos(t)^2 c_0(r, z) + \sin(t)^2 c_1(r, z)$$

$$c_0(r, z) = \exp\left(-\frac{(r - r_0)^2 + (z - z_0)^2}{\sigma_0}\right),$$

$$r_0 = 0, \quad z_0 = -0.6, \sigma_0 = 0.1$$

$$c_1(r, z) = \exp\left(-\frac{(r - r_1)^2 + (z - z_1)^2}{\sigma_1}\right),$$

$$r_1 = 0, \quad z_1 = -0.7, \sigma_1 = 0.1$$

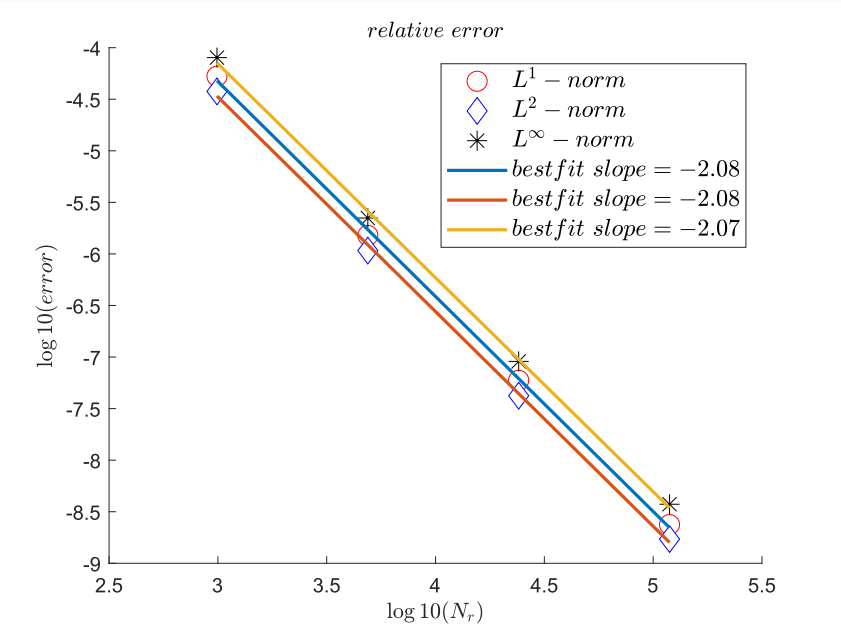

N_r	N_z	e_1, p_1	e_2, p_2	e_∞, p_∞
20	30	1.389E-02,	1.199E-02,	1.663E-02,
40	60	2.966E-03, 2.227	2.560E-03, 2.227	3.511E-03 , 2.244
80	120	7.276E-04, 2.027	6.265E-04, 2.031	8.742E-04, 2.006
160	240	1.796E-04, 2.018	1.561E-04, 2.005	2.188E-04, 1.998

Multigrid performance

Convergence factor ρ:

$$\rho^{(k+1)} = \frac{\left\| r_h^{(k+1)} \right\|}{\left\| r_h^{(k)} \right\|}$$

Optimal multigrid is achieved when $\rho^{(k+1)} \approx 0.1$.

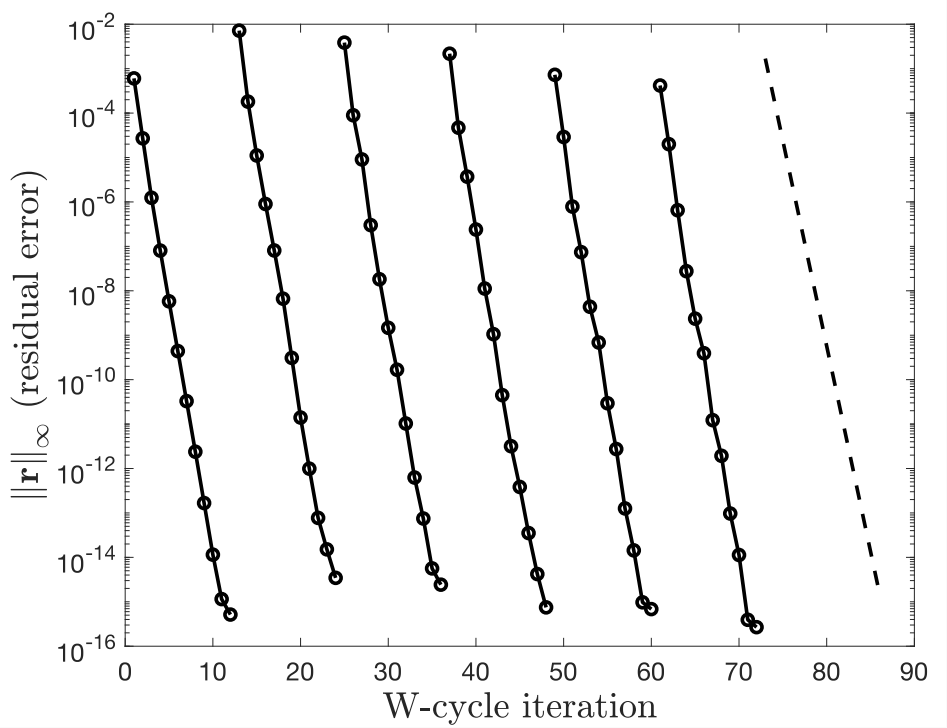

Section 4

Moving bubbles

Contents

Complete system

The main purpose of this work is to study the following system:
carrier concentration satisfies an advection-diffusion equation coupled with the Stokes equations

$$
\begin{aligned}
c_t &= \nabla \cdot \vec{J} \quad \text{in } \Omega \\
\vec{J} &= D\nabla c - c\vec{u} \quad \text{in } \Omega \\
\vec{J} \cdot \hat{n}_1 &= 0 \quad \text{on } \Gamma_{\mathcal{S}} \cup \Gamma_{\mathcal{C}} \\
M\frac{\partial c}{\partial t} &= MD\frac{\partial^2 c}{\partial \vec{\tau}^2} - D\frac{\partial c}{\partial \hat{n}_2} \quad \text{on } \Gamma_{\mathcal{B}}
\end{aligned}
$$

Complete system

The main purpose of this work is to study the following system:
carrier concentration satisfies an advection-diffusion equation coupled with the Stokes equations

$$c_t = \nabla \cdot \vec{J} \quad \text{in } \Omega$$

$$\vec{J} = D\nabla c - c\vec{u} \quad \text{in } \Omega$$

$$\vec{J} \cdot \hat{n}_1 = 0 \quad \text{on } \Gamma_{\mathcal{S}} \cup \Gamma_{\mathcal{C}}$$

$$M\frac{\partial c}{\partial t} = MD\frac{\partial^2 c}{\partial \vec{\tau}^2} - D\frac{\partial c}{\partial \hat{n}_2} \quad \text{on } \Gamma_{\mathcal{B}}$$

$$\vec{u}_t + \nabla p = \frac{1}{Re}\nabla^2 \vec{u} \quad \text{in } \Omega$$

$$\nabla \cdot \vec{u} = 0 \quad \text{in } \Omega$$

$$\vec{u} = 0 \quad \text{on } \Gamma_{\mathcal{S}}$$

$$\vec{u} = \vec{u}_B \quad \text{on } \Gamma_{\mathcal{B}}$$

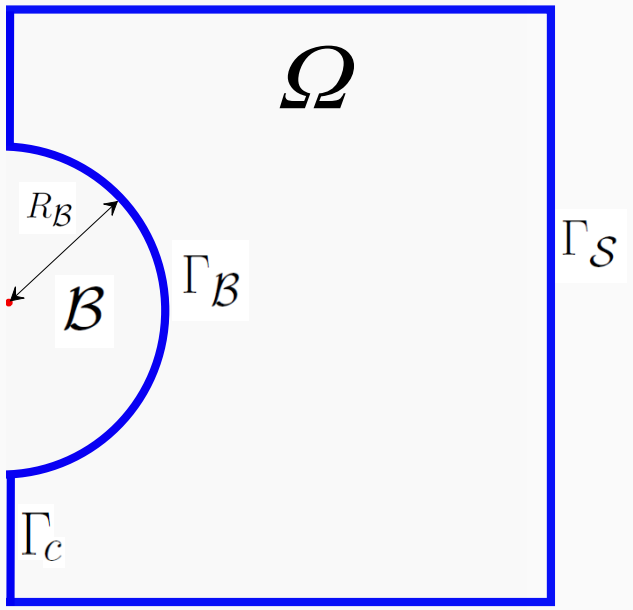

our unknowns: concentration c and the speed $\vec{u}$.

Stokes equations

The flow around an oscillating bubble is governed by the Incompressible Navier-Stokes equations. We assume external forces (gravity) are negligible.

$$\begin{aligned} \frac{\partial \vec{u}}{\partial t} + \vec{u} \cdot \nabla \vec{u} + \nabla p &= \frac{1}{Re} \nabla^2 \vec{u} \\ \nabla \cdot \vec{u} &= 0 \end{aligned}$$

Stokes equations

The flow around an oscillating bubble is governed by the Incompressible Navier-Stokes equations. We assume external forces (gravity) are negligible.

$$\begin{aligned} \frac{\partial \vec{u}}{\partial t} + \vec{u} \cdot \nabla \vec{u} + \nabla p &= \frac{1}{Re} \nabla^2 \vec{u} \\ \nabla \cdot \vec{u} &= 0 \end{aligned}$$

Assumption: small Reynolds number

- density is $\rho = 1000 \text{ kg/m}^3$
- viscosity is $\mu = 8.90 \cdot 10^{-4} \text{ Pa} \cdot \text{s}$
- amplitude is $A = 10^{-8} \text{ m}$
- frequency is $\nu = 10^3$
- typical distance is $\langle d \rangle = 10^{-3} \text{ m}$

Stokes equations

The flow around an oscillating bubble is governed by the Incompressible Navier-Stokes equations. We assume external forces (gravity) are negligible.

$$\begin{aligned} \frac{\partial \vec{u}}{\partial t} + \vec{u} \cdot \nabla \vec{u} + \nabla p &= \frac{1}{Re} \nabla^2 \vec{u} \\ \nabla \cdot \vec{u} &= 0 \end{aligned}$$

Assumption: small Reynolds number

- density is $\rho = 1000\ \mathrm{kg/m^3}$
- viscosity is $\mu = 8.90 \cdot 10^{-4}\ \mathrm{Pa \cdot s}$
- amplitude is $A = 10^{-8}\ \mathrm{m}$
- frequency is $\nu = 10^3$
- typical distance is $\langle d \rangle = 10^{-3}\ \mathrm{m}$

$\Longrightarrow$

Typical Reynolds number is therefore ($\langle v \rangle = A\,\omega = A\,2\pi\,\nu$):

$$Re = \frac{\rho \langle v \rangle \langle d \rangle}{\mu} = \frac{\rho A\, 2\pi\, \nu\, \langle d \rangle}{\mu} < 0.1$$

Stokes equations

The flow around an oscillating bubble is governed by the Incompressible Navier-Stokes equations. We assume external forces (gravity) are negligible.

$$\begin{aligned} \frac{\partial \vec{u}}{\partial t} + \vec{u} \cdot \nabla \vec{u} + \nabla p &= \frac{1}{Re} \nabla^2 \vec{u} \\ \nabla \cdot \vec{u} &= 0 \end{aligned}$$

Assumption: small Reynolds number

- density is $\rho = 1000\ \mathrm{kg/m^3}$
- viscosity is $\mu = 8.90 \cdot 10^{-4}\ \mathrm{Pa \cdot s}$
- amplitude is $A = 10^{-8}\ \mathrm{m}$
- frequency is $\nu = 10^3$
- typical distance is $\langle d \rangle = 10^{-3}\ \mathrm{m}$

$\Longrightarrow$

Typical Reynolds number is therefore ($\langle v \rangle = A\,\omega = A\,2\pi\,\nu$):

$$Re = \frac{\rho \langle v \rangle \langle d \rangle}{\mu} = \frac{\rho A\, 2\pi\, \nu\, \langle d \rangle}{\mu} < 0.1$$

$\Longrightarrow$ convective term are neglected ($\vec{u} \cdot \nabla \vec{u} = 0$)

Discretization in space: MAC grid

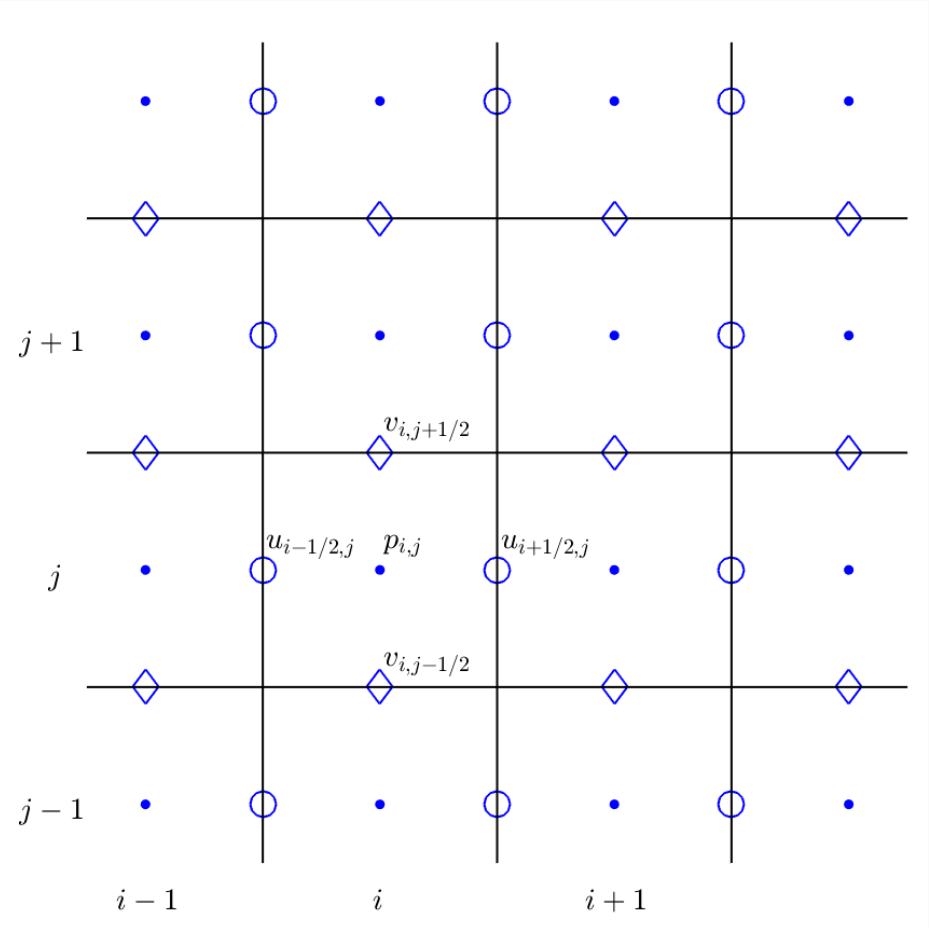

u is defined in ○

v is defined in ◇

p is defined in •

The *MAC* grid is used to avoid the checkboard instability for the pressure term observed in non-staggered grids due to the fact that p appears in the equations only in the form of ∇p.

Discretization in time

Finally, the equation reads: $\frac{\partial \vec{u}}{\partial t} + \nabla p = \frac{1}{Re} \nabla^2 \vec{u}$.

Discretization in time

Finally, the equation reads: $\frac{\partial \vec{u}}{\partial t} + \nabla p = \frac{1}{Re}\nabla^2 \vec{u}$. A popular approach for time discretization is the **Projection method**:

$$\frac{\vec{u}^* - \vec{u}^n}{\Delta t} = \frac{1}{Re}\nabla^2 \vec{u}^*$$
$$\vec{u}^{n+1} = \vec{u}^* - \nabla \chi^{n+1} \tag{9}$$

Taking divergence of both sides of (9): $\nabla^2 \chi^{n+1} = \nabla \cdot \vec{u}^*$

Boundary conditions: Projecting (9) to the boundary:

$$\vec{u}_b \cdot \vec{n} = \vec{u}^* \cdot \vec{n} - \nabla \chi^{n+1} \cdot \vec{n} \qquad \vec{u}_b \cdot \vec{\tau} = \vec{u}^* \cdot \vec{\tau} - \nabla \chi^{n+1} \cdot \vec{\tau}$$

Discretization in time

Finally, the equation reads: $\frac{\partial \vec{u}}{\partial t} + \nabla p = \frac{1}{Re}\nabla^2 \vec{u}$. A popular approach for time discretization is the **Projection method**:

$$\frac{\vec{u}^* - \vec{u}^n}{\Delta t} = \frac{1}{Re}\nabla^2 \vec{u}^*$$
$$\vec{u}^{n+1} = \vec{u}^* - \nabla \chi^{n+1} \tag{9}$$

Taking divergence of both sides of (9): $\nabla^2 \chi^{n+1} = \nabla \cdot \vec{u}^*$

Boundary conditions: Projecting (9) to the boundary:

$$\vec{u}_b \cdot \vec{n} = \vec{u}^* \cdot \vec{n} - \nabla \chi^{n+1} \cdot \vec{n} \qquad \vec{u}_b \cdot \vec{\tau} = \vec{u}^* \cdot \vec{\tau} - \nabla \chi^{n+1} \cdot \vec{\tau}$$

One possible choice of boundary conditions for χ^{n+1} and $\vec{u}^*$ is:

$$\begin{aligned}
\frac{\partial \chi^{n+1}}{\partial \vec{n}} &= 0 \\
\vec{u}^* \cdot \vec{n} &= \vec{u}_b \cdot \vec{n} \\
\vec{u}^* \cdot \vec{\tau} &= \vec{u}_b \cdot \vec{\tau} + \frac{\partial \tilde{\chi}^{n+1}}{\partial \vec{\tau}} \\
\tilde{\chi}^{n+1} &= 2\chi^n - \chi^{n-1}
\end{aligned}$$

Pros: three elliptic equations to solve at each time step

Cons: divergence is only first order accurate (i.e. $\nabla \cdot \vec{u} = \mathcal{O}(h)$)

Discretization in time

An alternative approach is represented by:

Crank-Nicolson (monolithic method)

$$
\begin{aligned}
\frac{\vec{u}^{n+1} - \vec{u}^{n}}{\Delta t} + \nabla p^{n+1/2} &= \frac{1}{2\,Re}\left(\nabla^2 \vec{u}^{n+1} + \nabla^2 \vec{u}^{n}\right) \\
\nabla \cdot \vec{u}^{n+1} &= 0 \\
\vec{u}^{n+1} &= \vec{u}_b \qquad \text{on } \partial\mathcal{B}(0)
\end{aligned}
$$

Discretization in time

An alternative approach is represented by:

Crank-Nicolson (monolithic method)

$$
\begin{aligned}
\frac{\vec{u}^{n+1} - \vec{u}^{n}}{\Delta t} + \nabla p^{n+1/2} &= \frac{1}{2\,Re}\left(\nabla^2 \vec{u}^{n+1} + \nabla^2 \vec{u}^{n}\right) \\
\nabla \cdot \vec{u}^{n+1} &= 0 \\
\vec{u}^{n+1} &= \vec{u}_b \qquad \text{on } \partial\mathcal{B}(0)
\end{aligned}
$$

Pros: second order accuracy in $\vec{u}$ and $\nabla \cdot \vec{u}$

Cons 1: pressure in not uniquely defined (the discretized linear system is singular)

Cons 2: leading to a much larger linear system, (whose unknowns are $(u^{n+1}, v^{n+1}, p^{n+1/2})$)

Cons 1: pressure in not uniquely defined $\Longrightarrow$ stabilization technique

The problem is augmented by introducing an additional unknown $\xi^{n+1} \in \mathbb{R}$ and an equation for $p^{n+1/2}$:

$$
\begin{aligned}
\frac{\vec{u}^{n+1} - \vec{u}^{n}}{\Delta t} + \nabla p^{n+1/2} &= \frac{1}{2\,Re}\left(\nabla^2 \vec{u}^{n+1} + \nabla^2 \vec{u}^{n}\right) \\
\nabla \cdot \vec{u}^{n+1} &= \xi^{n+1} \\
\vec{u}^{n+1} &= \vec{u}_b \qquad \text{on } \partial\mathcal{B}(0) \\
\sum p_{ij}^{n+1/2} &= 0
\end{aligned}
$$

Remark: Observe that no b.c. for $p^{n+1/2}$ are required.

Cons 1: pressure in not uniquely defined $\Longrightarrow$ stabilization technique

The problem is augmented by introducing an additional unknown $\xi^{n+1} \in \mathbb{R}$ and an equation for $p^{n+1/2}$:

$$
\begin{aligned}
\frac{\vec{u}^{n+1} - \vec{u}^{n}}{\Delta t} + \nabla p^{n+1/2} &= \frac{1}{2\,Re}\left(\nabla^2 \vec{u}^{n+1} + \nabla^2 \vec{u}^{n}\right) \\
\nabla \cdot \vec{u}^{n+1} &= \xi^{n+1} \\
\vec{u}^{n+1} &= \vec{u}_b \qquad \text{on } \partial\mathcal{B}(0) \\
\sum p_{ij}^{n+1/2} &= 0
\end{aligned}
$$

Remark: Observe that no b.c. for $p^{n+1/2}$ are required.

Cons 2: large linear system $\Longrightarrow$ **multigrid**

Crank-Nicolson (monolithic method)

Cons 1: pressure in not uniquely defined $\Longrightarrow$ stabilization technique

The problem is augmented by introducing an additional unknown $\xi^{n+1} \in \mathbb{R}$ and an equation for $p^{n+1/2}$:

$$
\begin{aligned}
\frac{\vec{u}^{n+1} - \vec{u}^{n}}{\Delta t} + \nabla p^{n+1/2} &= \frac{1}{2\,Re}\left(\nabla^2 \vec{u}^{n+1} + \nabla^2 \vec{u}^{n}\right) \\
\nabla \cdot \vec{u}^{n+1} &= \xi^{n+1} \\
\vec{u}^{n+1} &= \vec{u}_b \qquad \text{on } \Gamma_{\mathcal{B}} \\
\sum p_{ij}^{n+1/2} &= 0
\end{aligned}
$$

Cons 2: the additional equation is balanced with the additional unknown ξ that decays to zero with the order of the method

Remark: Observe that no b.c. for $p^{n+1/2}$ are required.

Test 1: pulsating bubble

In this test we model the expansion/compression of a (pulsating) bubble, represented by a sphere $\mathcal{B}(t)$ centred at the origin and with radius:

$$R(t) = R_{\mathcal{B}}(1 + A\sin(\omega t))$$

where $R_{\mathcal{B}} = R(0)$, A the amplitude, $\omega = 2\pi\nu$ and ν the frequency. The velocity of the bubble surface is

$$\mathbf{u}_b(\xi, z) = R'(t)\,\mathbf{n} = A\,R_{\mathcal{B}}\,\omega\cos(\omega\,t)\,\mathbf{n}$$

where $\mathbf{n} = (\xi, z)/\sqrt{\xi^2 + z^2}$ and $\sqrt{\xi^2 + z^2} = R(t)$.
The exact solution for the 3D axisymmetric Stokes problem with free-slip boundary conditions on the bubble surface in a semi-infinite domain $\Omega(t) = \{(\xi, z)\colon 0 < \xi < +\infty,\ \ \xi^2 + z^2 > (R(t))^2\}$ is:

$$\mathbf{u}_{\text{exa}} = R'(t)\frac{(R(t))^2}{(\xi^2 + z^2)^{3/2}} \cdot (\xi, z), \quad p = R(t)(R''(t)R(t) + 2(R'(t))^2)/\sqrt{\xi^2 + z^2}.$$

Accuracy test

Remark

In a finite domain we cannot prescribe the wall boundary conditions $\mathbf{u} = 0$ on the external boundary otherwise the mass conservation is not guaranteed $\Longrightarrow$ we prescribe the exact velocity at $\Gamma_{\mathcal{S}}$

We choose $R_{\mathcal{B}} = 0.253$, $A = 0.04$, $\omega = 2\pi\,\nu$, $\nu = 50$ and $t_{fin} = 0.1$.

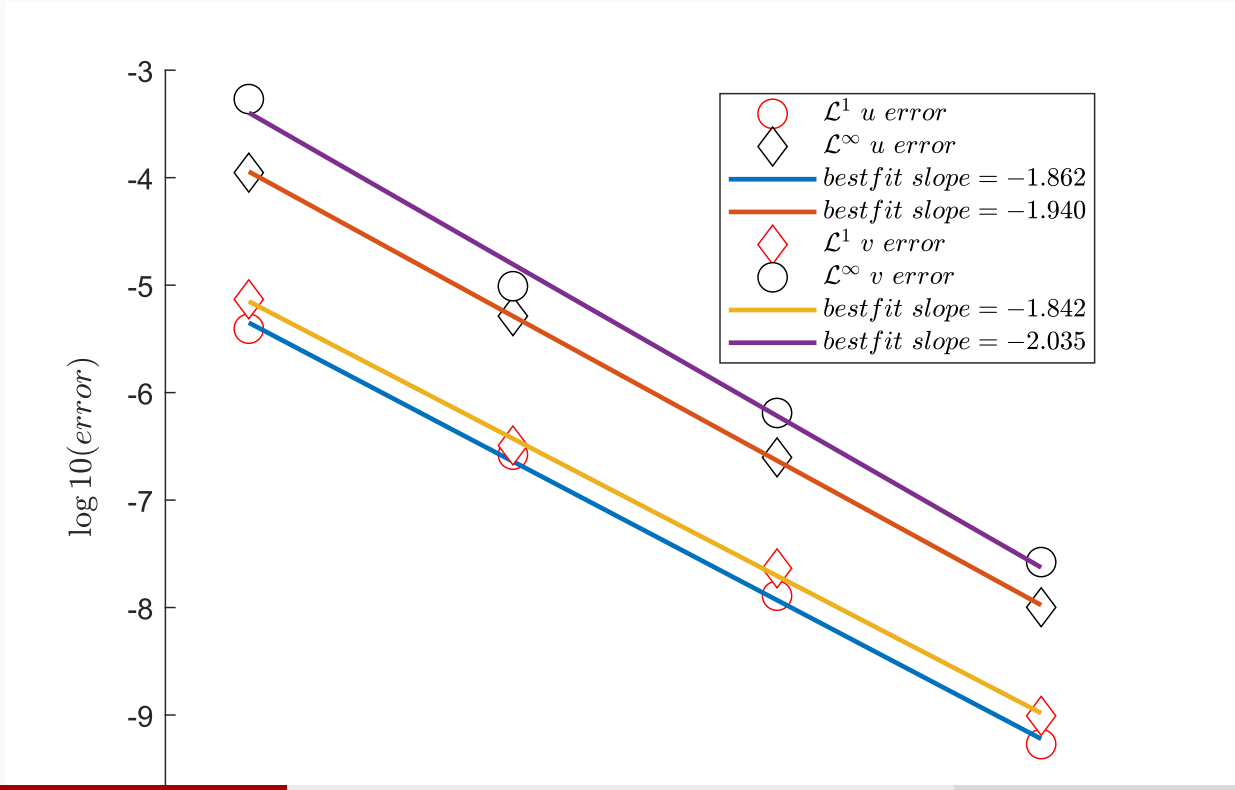

Steady vs moving computational bubble

When the amplitude of the bubble oscillation is sufficiently small compared to the spatial step, $R(t) \approx R_{\mathcal{B}}$, it is reasonable to simplify the model by assuming that the velocity of the surface bubble is assigned:

$$\mathbf{u}_b(\xi, z) = A\,\omega\cos(\omega\,t)(\xi, z) \text{ for } \sqrt{\xi^2 + z^2} = R_{\mathcal{B}}.$$

In this way, the computational domain does not move on time and the exact solution is:

$$\mathbf{u}^{\mathrm{f}}_{\mathrm{exa}} = R'(t)\frac{(R_{\mathcal{B}})^2}{(\xi^2 + z^2)^{3/2}} \cdot (\xi, z), \quad p = R''(t)R_{\mathcal{B}}^2/\sqrt{\xi^2 + z^2}.$$

Numerical results

The difference between the exact solutions is

$$\mathbf{u}_{\text{exa}} - \mathbf{u}^{\text{f}}_{\text{exa}} = \mathcal{O}(A)$$

$\Longrightarrow$ the difference between the two approaches decays as $A \to 0$.

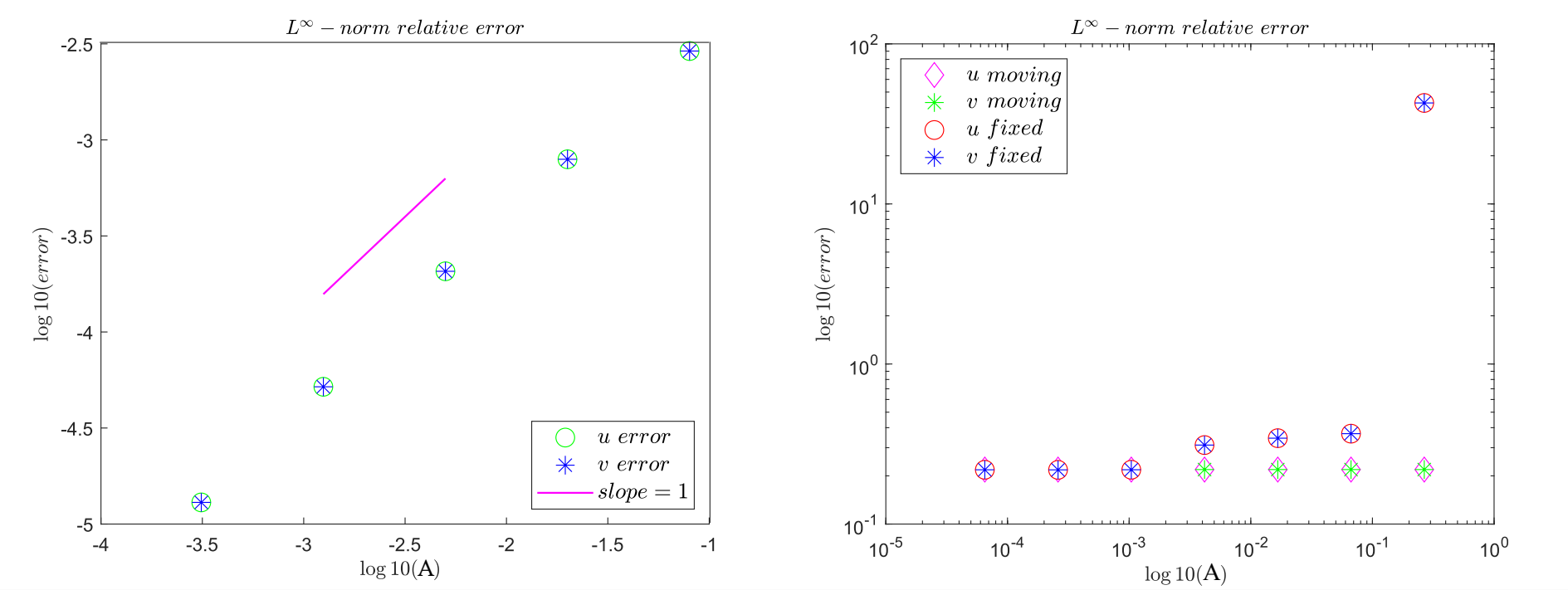

Figure 2: *Left panel: relative error between the two numerical solutions* $\mathbf{u}_h, \mathbf{u}^f_h$. *Right panel: relative error between* $\mathbf{u}_h, \mathbf{u}_{exa}$ *and* $\mathbf{u}^f_h, \mathbf{u}^f_{exa}$.

Harmonic vertical oscillation of the spherical bubble: $\nu = 10$

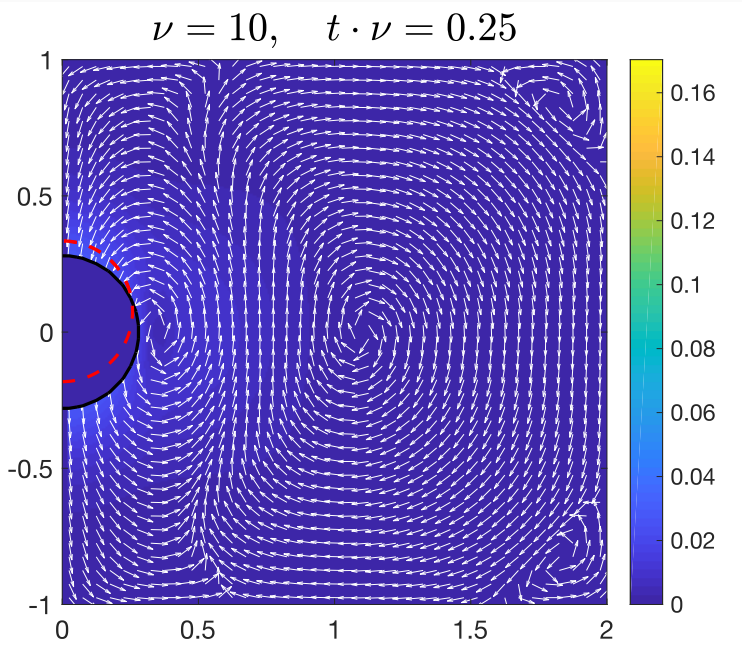

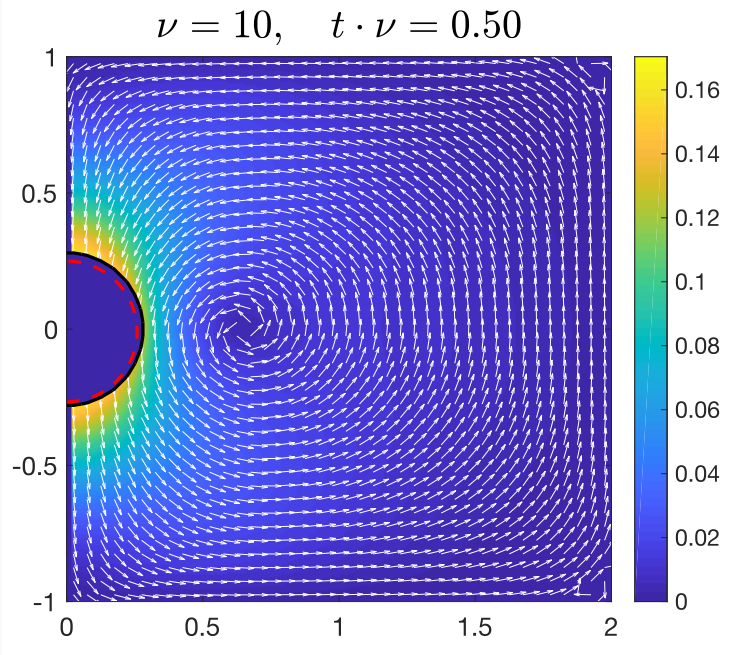

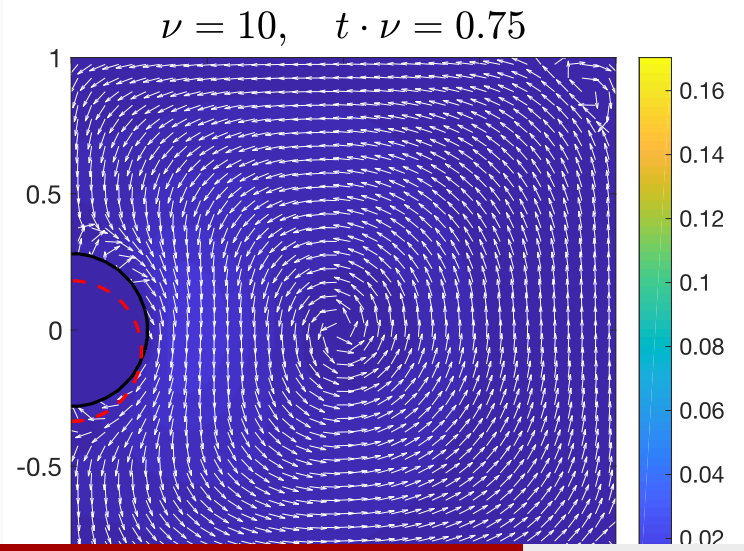

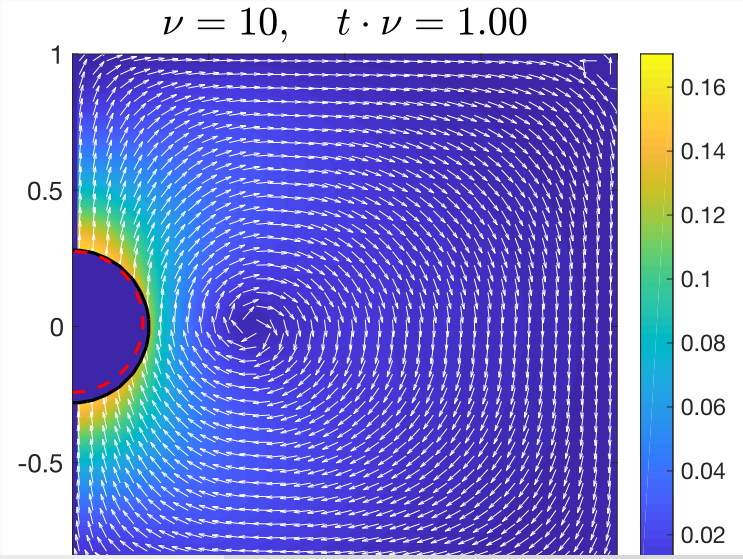

Harmonic vertical oscillation of the spherical bubble: $\nu = 20$

https://www.youtube.com/watch?v=YueQeDZqC9o

Harmonic vertical oscillation of the spherical bubble: $\nu = 2422$

https://www.youtube.com/watch?v=-SeBaXRZtXY

Ellipsoidal deformation of the bubble: $\nu = 10$

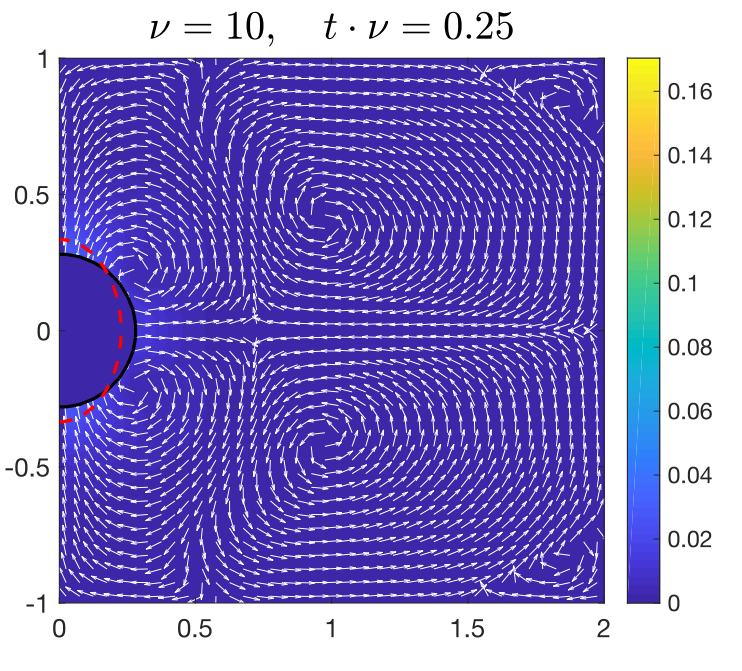

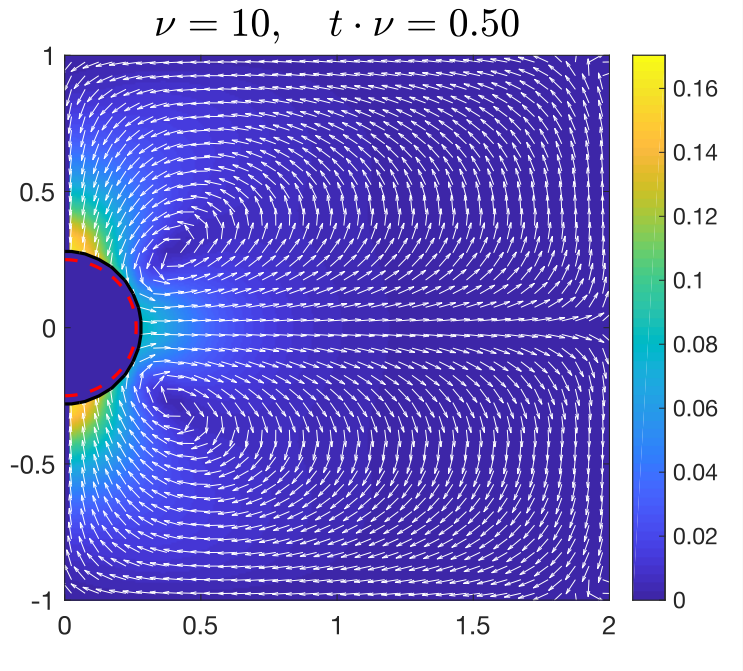

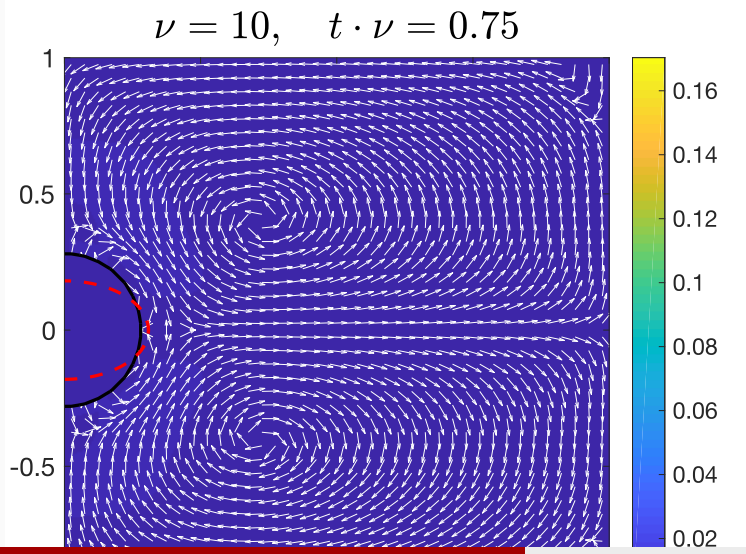

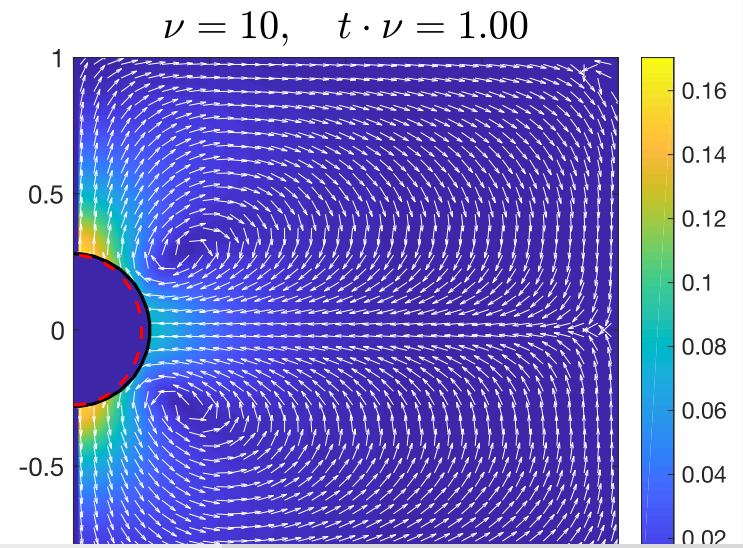

Ellipsoidal deformation of the bubble: $\nu = 20$

https://www.youtube.com/watch?v=PnF6CdtZ89U

Ellipsoidal deformation of the bubble: $\nu = 2422$

https://www.youtube.com/watch?v=lQOxep9H7Zs

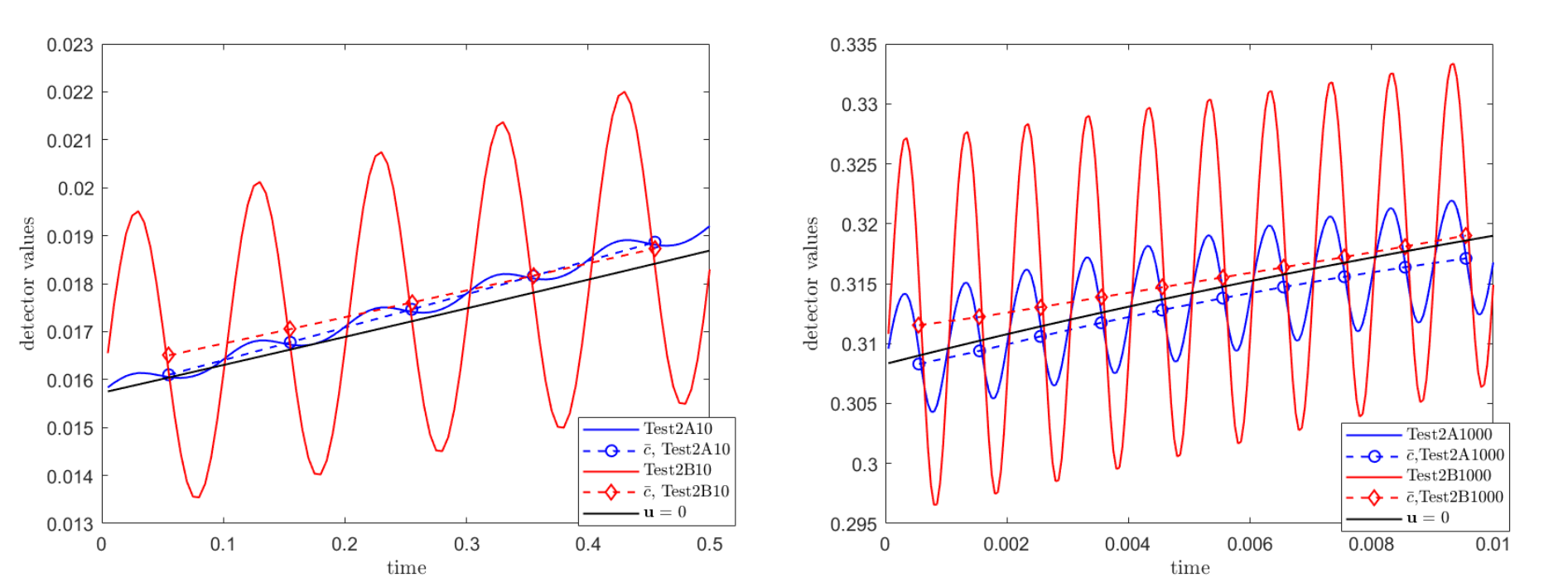

Figure 3: *Detector values of the particle concentration c at $(\xi_d = 0.4, z_d = 0)$. The spatial step is $h = 1/120$. On the left we plot the comparison between* TEST2A10 *(blue line),* TEST2B10 *(red line) and steady-bubble case with $\mathbf{u} = 0$ (black line). Analogously, on the right, we show the comparison between* TEST2A1000 *and* TEST2B1000*. The dashed lines represent the mean values of the respective tests.*

Section 5

Conclusion

Contents

Summary and future projects

Summary and future projects

$\surd$ Spatial multiscale challenge is solved

Summary and future projects

- $\surd$ Spatial multiscale challenge is solved
- $\surd$ Second order method in space and time for Stokes equations

Summary and future projects

- $\surd$ Spatial multiscale challenge is solved
- $\surd$ Second order method in space and time for Stokes equations
- $\surd$ Comparison between moving and static domain for small oscillations

Summary and future projects

- $\surd$ Spatial multiscale challenge is solved
- $\surd$ Second order method in space and time for Stokes equations
- $\surd$ Comparison between moving and static domain for small oscillations
- $\surd$ Coupling the Stokes equation with the advection-diffusion equation

Summary and future projects

- √ Spatial multiscale challenge is solved
- √ Second order method in space and time for Stokes equations
- √ Comparison between moving and static domain for small oscillations
- √ Coupling the Stokes equation with the advection-diffusion equation
- ? Spatial multiscale challenge is solved

References... and thank you for the attention

- Clarissa Astuto, Armando Coco, and Giovanni Russo, *A finite-difference ghost-point multigrid method for multi-scale modelling of sorption kinetics of a surfactant past an oscillating bubble*, Journal of Computational Physics (2023), 111880.
- Clarissa Astuto, Antonio Raudino, and Giovanni Russo, *Multiscale modeling of sorption kinetics*, arXiv preprint arXiv:2202.02552 (2022).
- Armando Coco, Mariarosa Mazza, and Matteo Semplice, *A ghost-point smoothing strategy for geometric multigrid on curved boundaries*, Journal of Computational Physics (2023), 111982.
- Armando Coco, *A multigrid ghost-point level-set method for incompressible navier-stokes equations on moving domains with curved boundaries*, Journal of Computational Physics **418** (2020), 109623.
- Armando Coco and Giovanni Russo, *Finite-difference ghost-point multigrid methods on cartesian grids for elliptic problems in arbitrary domains*, Journal of Computational Physics **241** (2013), 464–501.
- Armando Coco and Giovanni Russo, *Second order finite-difference ghost-point multigrid methods for elliptic problems with discontinuous coefficients on an arbitrary interface*, Journal of Computational Physics **361** (2018), 299–330.

Thank you for the attention